Regulation of the G2–M cell cycle progression by the ERK5–NFκB signaling pathway

Kelly Cude,[1] Yupeng Wang,[2] Hyun-Jung Choi,[2] Shih-Ling Hsuan,[2] Honglai Zhang,[3] Cun-Yu Wang,[3] and Zhengui Xia[1,2]

[1]Graduate Program in Molecular and Cellular Biology and [2]Department of Environmental and Occupational Health Sciences, University of Washington, Seattle, WA 98195
[3]Department of Biologic and Materials Sciences, University of Michigan, Ann Arbor, MI 48109

Elucidation of mechanisms regulating cell cycle progression is of fundamental importance for cell and cancer biology. Although several genes and signaling pathways are implicated in G1–S regulation, less is known regarding the mechanisms controlling cell cycle progression through G2 and M phases. We report that extracellular signal–regulated kinase 5 (ERK5), a member of the mitogen-activated protein kinases, is activated at G2–M and required for timely mitotic entry. Stimulation of ERK5 activated nuclear factor κB (NFκB) through ribosomal S6 kinase 2 (RSK2)-mediated phosphorylation and degradation of IκB. Furthermore, selective inhibition of NFκB at G2–M phases substantially delayed mitotic entry and inhibited transcription of G2–M–specific genes, including cyclin B1, cyclin B2, Plk-1, and cdc25B. Moreover, inhibition of NFκB at G2–M diminished mitosis induced by constitutive activation of ERK5, providing a direct link between ERK5, NFκB, and regulation of G2–M progression. We conclude that a novel ERK5–NFκB signaling pathway plays a key role in regulation of the G2–M progression.

Introduction

The extracellular signal–regulated kinase (ERK) 5 is a member of the MAPKs (Lee et al., 1995; Zhou et al., 1995). The N-terminal kinase domain of ERK5 is highly homologous to the prototypical MAPKs ERK1/2. However, ERK5 is selectively activated by its upstream kinase MEK5 (English et al., 1995) and ERK5-null mice are embryonic lethal (Hayashi and Lee, 2004), suggesting that ERK5 has unique biological functions that cannot be compensated for by ERK1/2. Stimulation of ERK5 regulates neuronal survival, muscle cell differentiation, and cellular proliferation and transformation (Kato et al., 1998; Pearson et al., 2001; Watson et al., 2001; Liu et al., 2003; Shalizi et al., 2003). Hyperactivity of the ERK5 pathway is associated with highly aggressive forms of breast and prostate cancers (Esparis-Ogando et al., 2002; Mehta et al., 2003).

Mechanisms for ERK5 regulation of proliferation are not well understood. However, several targets of ERK5 have been identified, including nuclear factor κB (NFκB), c-myc, and cyclin D, all of which are potential regulators of proliferation (Wang and Tournier, 2006). NFκB is of particular interest because it regulates the G1–S transition of the cell cycle and is required for oncogenic transformation by Ras (Finco et al., 1997; Hinz et al., 1999). Mutations that result in constitutive activation of NFκB are common in epithelial tumors, tumor cell lines, and lymphoid malignancies. These NFκB mutations cause increased proliferation rates and metastatic capacity (Karin et al., 2002). Interestingly, ERK5-mediated activation of NFκB promotes cellular transformation in NIH 3T3 cells (Pearson et al., 2001).

To elucidate mechanisms for ERK5 regulation of cellular proliferation, we investigated the importance of ERK5 in cell cycle progression. We examined ERK5 activity at different stages of the cell cycle and discovered that ERK5 is activated in a cell cycle–dependent manner, with maximal activation at G2–M. Evidence is presented supporting a critical role for ERK5 in the G2–M progression. Our data also identify NFκB-mediated transcription as a key downstream mechanism by which ERK5 regulates the G2–M phase transition.

Results

ERK5 is activated during the G2–M phases of the cell cycle

Although ERK5 plays a pivotal role in growth factor–induced cellular proliferation (Kato et al., 1998), its role in cell cycle

K. Cude and Y. Wang contributed equally to this paper.

Correspondence to Zhengui Xia: zxia@u.washington.edu

Abbreviations used in this paper: ca, constitutive-active; dn, dominant-negative; ERK, extracellular signal–regulated kinase; HFF, human foreskin fibroblast; hSMC, human artery smooth muscle cell; MBP, myelin basic protein; NFκB, nuclear factor κB; Plk, polo-like kinase; RSK, ribosomal S6 kinase; SR, super repressor; wt, wild-type.

The Journal of Cell Biology, Vol. 177, No. 2, April 23, 2007 253–264
http://www.jcb.org/cgi/doi/10.1083/jcb.200609166

regulation is unclear. To determine whether ERK5 is activated at specific stages of the cell cycle, Western analysis using an anti-ERK5 antibody was performed on HeLa cells arrested at different stages of the cell cycle. The cell cycle stage for each treatment was confirmed by flow cytometry analysis (FACS; Fig. 1 A and not depicted). Cell cycle arrest at M phase was further confirmed by Western analysis and immunostaining using an antibody that recognizes phosphorylated mitosis-specific marker proteins (p-MPM-2; Fig. 1, A and B). Treatment of cells with the microtubule destabilizing agent nocodazole, which arrests cells at the start of the M phase, caused a reduced electrophoretic mobility (phosphorylation shift) of ERK5 (Fig. 1 A), indicative of ERK5 activation (Kato et al., 1998). In contrast to M phase arrest, there was very little activation of ERK5 in asynchronized cells or when cells were arrested at G1, S, or the G1–S boundary of the cell cycle (Fig. 1, A and D).

Nocodazole activation of ERK5 was apparently due to the arrest of cells at M phase. Arrest of HeLa cells at M phase with taxol also caused ERK5 activation (unpublished data). In addition, we treated primary cultured cortical neurons from newborn rats with nocodazole. In contrast to HeLa cells, nocodazole did not induce ERK5 phosphorylation in these postmitotic cortical neurons, although these cells express abundant ERK5 that is readily activated by brain-derived neurotrophic factor (Fig. 1 C). Moreover, we collected mitotic HeLa cells by shaking them off the culture dish 9 h after thymidine release (mitotic; Fig. 1 D). ERK5 was phosphorylated in this highly enriched mitotic cell population but not in nonmitotic control cells. Finally, ERK5 activation in mitotic and in nocodazole-arrested M phase HeLa cells was confirmed by a direct kinase assay (Fig. 1 D). MEK5, the only known kinase that phosphorylates and activates ERK5 (English et al., 1995), was also activated in mitotic and nocodazole-treated HeLa cells (Fig. 1 E).

We also measured ERK5 activation as S phase–synchronized HeLa cells progressed to M phase. When HeLa cells were released from a single-thymidine block that synchronizes cells at early S phase, ERK5 phosphorylation was detectable 6 h after thymidine release. At this time, there was a small increase in the number of cells harboring 4n DNA but very few mitotic cells (Fig. 2, A–C). Mitotic cells were identified by both positive immunostaining of p-MPM-2 and the condensed nuclear morphology typical of mitotic cells (Fig. 1 B). ERK5 phosphorylation peaked 8 h after release from a single-thymidine block, when the majority of cells (>84%) had 4n DNA content, but only 5% of the cells were mitotic. Similar observations were made when HeLa cells were synchronized with a double-thymidine block (Fig. 2, D–F). ERK5 phosphorylation was readily detectable 9 h after thymidine release, a time when the majority of cells

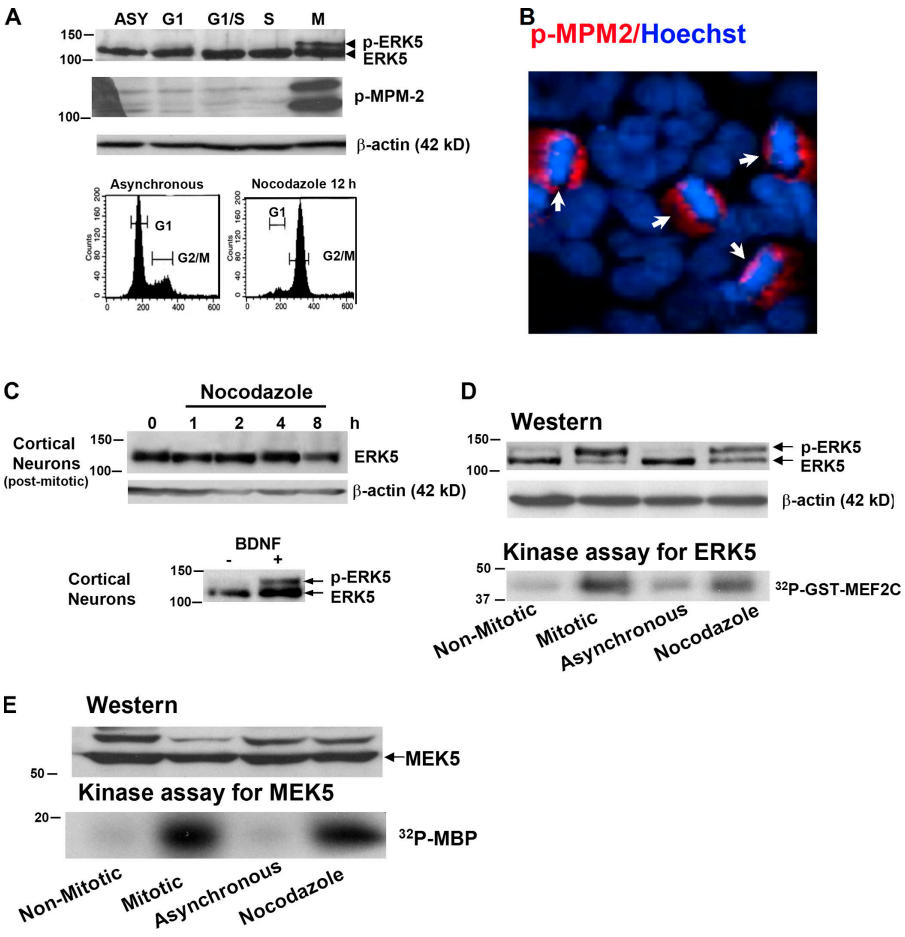

Figure 1. **ERK5 is activated during G2–M phases of the cell cycle.** (A) ERK5 is activated in a cell cycle–dependent manner. HeLa cells were treated with cell cycle–arresting drugs described in Materials and methods or left untreated as an asynchronous (ASY) population. M phase arrest was verified by Western analysis for p-MPM-2 and by FACS analysis of DNA content. Cell lysates were prepared for Western analysis using a polyclonal antibody against ERK5. Phosphorylated ERK5 appears as a shift in ERK5 mobility, indicative of ERK5 activation. β-Actin was used as a loading control. (B) Mitotic cells are identified by positive p-MPM-2 staining (red), and condensed nuclear morphology was visualized after staining with Hoechst 33342 (blue). (C) 0.5 μg/ml nocodazole treatment does not induce ERK5 phosphorylation in postmitotic neurons cultured from newborn rat cortex, suggesting that ERK5 activation by nocodazole is specific to cycling cells. Brain-derived neurotrophic factor (BDNF) stimulation of ERK5 phosphorylation was used as a positive control for ERK5 in cortical neurons. (D) The kinase activity of ERK5 is stimulated in mitotic and nocodazole-treated HeLa cells. Mitotic cells were gently shaken off the tissue culture flasks and collected 9 h after release from a double-thymidine block. The cells remaining attached to the flasks were collected as a "nonmitotic" control. HeLa cells were also treated with 0.5 μg/ml nocodazole for 12 h or vehicle as an asynchronous control. Cell lysates were subjected to Western analysis for ERK5 and β-actin (top) or an immunoprecipitation-coupled in vitro kinase assay for ERK5 using GST-MEF2C as a substrate (bottom). (E) The kinase activity of MEK5 is stimulated in mitotic and nocodazole-treated HeLa cells. Cell lysates were collected as in D and subjected to Western analysis for MEK5 as loading control (top) or an immunoprecipitation-coupled in vitro kinase assay for MEK5 using MBP as a substrate (bottom). The anti-MEK5 antibody also cross-reacted nonspecifically with a protein band above MEK5.

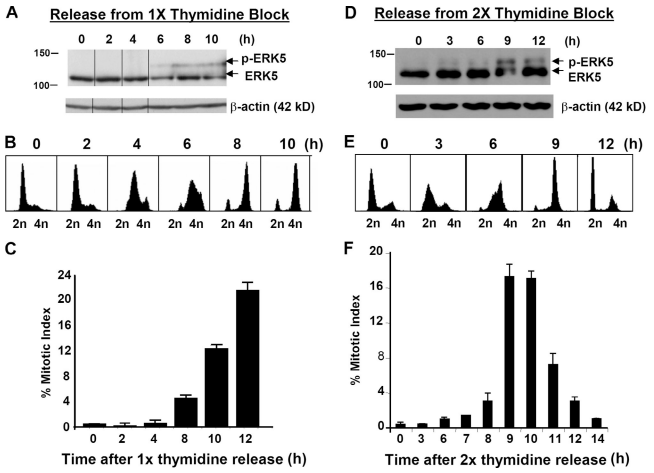

Figure 2. **ERK5 is activated when HeLa cells enter G2–M after release from a thymidine block.** HeLa cells were released from a single- (A–C) or double- (D–F) thymidine block. (A and D) Western analysis showing ERK5 phosphorylation as cells enter G2–M. (B and E) FACS analysis for 2n and 4n DNA content after thymidine release. (C and F) Percentage of mitotic index (i.e., percentage of mitotic cells). Data are presented as means ± SEM.

(>86%) were in G2–M phases harboring 4n DNA, whereas only 17% of the cells were p-MPM-2$^+$ mitotic cells. We conclude that ERK5 is activated at both G2 and M phases.

ERK5 is critical for G2–M progression

The temporal profile of ERK5 activation suggests that it might play a role in G2–M progression. To test this hypothesis, we expressed various constructs that either activate or inhibit ERK5 signaling and evaluated their effects on mitosis. Expression of constitutive-active (ca) MEK5 with wild-type (wt) ERK5 in HeLa cells, which activates ERK5 in transfected cells, increased the number of cells that are positive for the mitotic markers p-MPM-2 and p-histone H3 (Fig. 3 A). These cells also displayed the typical mitotic nuclear morphology (unpublished data). This suggests that ectopic activation of ERK5 signaling is sufficient to increase mitotic index in an asynchronous population.

In a separate set of experiments, HeLa cells were transfected as in Fig. 3 A and treated 24 h after transfection with thymidine to synchronize cells at S phase. The mitotic index in the transfected cell population was determined 12 h after thymidine release. Constitutive activation of ERK5 significantly increased the mitotic index (Fig. 3 B), suggesting that more of these cells progressed from S phase into the mitotic phase. In contrast, transient expression of dominant-negative (dn) ERK5, which blocks ERK5 signaling, reduced the mitotic index. A similar experiment was performed using siRNA to suppress ERK5 expression and inhibit ERK5 signaling (Fig. 3 C). Transfection of the ERK5 siRNA greatly reduced ERK5 expression 48 h later (Fig. 3 C, top). When HeLa cells were synchronized by thymidine treatment

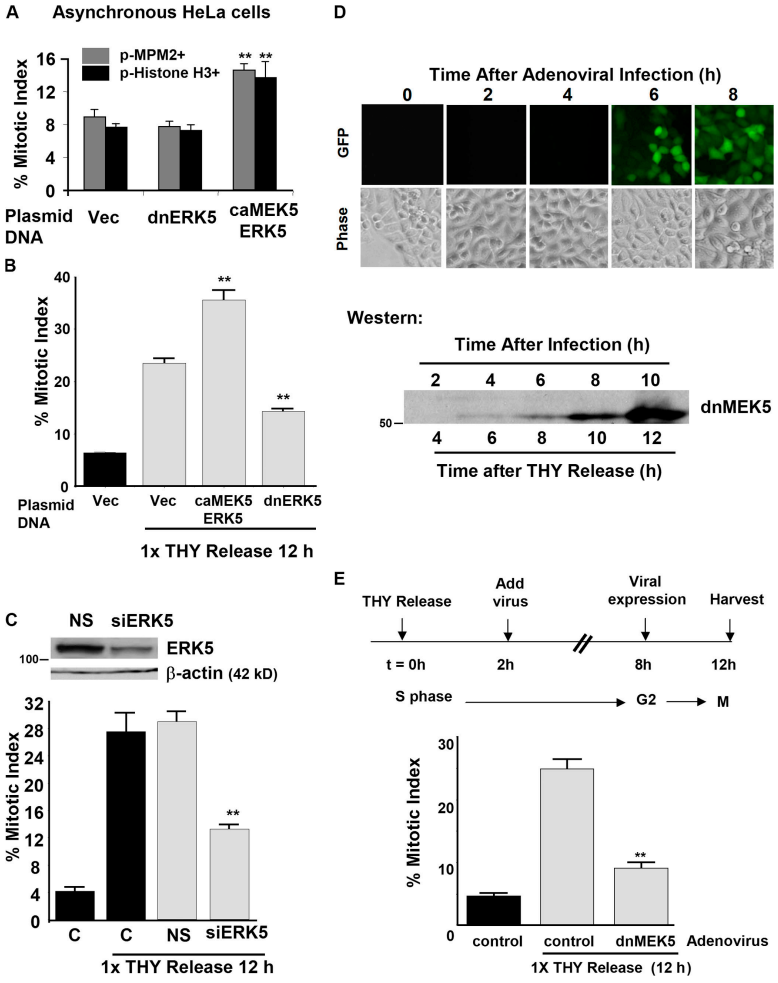

Figure 3. **ERK5 is critical for G2–M progression.** (A) Constitutive activation of ERK5 is sufficient to increase mitotic index in asynchronous HeLa cells. HeLa cells were transfected with plasmid DNA encoding caMEK5 + wtERK5 to activate ERK5. The vector control (Vec) or dnERK5 were used as controls. Cells were also cotransfected with EGFP to identify transfected cells. Mitotic cells in the transfected cell population (GFP$^+$) were identified 48 h after transfection by both condensed mitotic nuclear morphology and positive staining for mitotic markers p-MPM-2 or p-histone H3. (B) Constitutive activation of ERK5 increases, whereas blocking ERK5 reduces, mitotic index. HeLa cells were transfected with plasmid DNA as in A. Cells were treated 24 h later with thymidine for 14–16 h to synchronize at S phase. Mitotic index in transfected cells (GFP$^+$) was quantified 12 h after thymidine release. (C) siRNA silencing of ERK5 inhibits mitosis in transfected cells (GFP$^+$). HeLa cells were transfected with an ERK5 siRNA (siERK5) or a control nonsilencing siRNA (NS). A mock transfection (C) was included as a negative control. Anti-ERK5 Western analysis illustrates siRNA suppression of ERK5 protein 48 h after transfection. (D) Time course for adenoviral expression of GFP and dnMEK5. HeLa cells were synchronized at S phase with thymidine and then infected with an adenovirus expressing both GFP and dnMEK5 under separate promoters 2 h after thymidine release. GFP expression was detected by GFP fluorescence, whereas dnMEK5 expression was detected by Western analysis. (E) Adenoviral inhibition of ERK5 at G2–M reduces mitotic index. HeLa cells were released from a thymidine block and infected with dnMEK5 or a control adenovirus 2 h later. The mitotic index in adenovirus-infected cells (GFP$^+$) was determined 12 h after the second thymidine release (i.e., 10 h after infection). Data are presented as means ± SEM. **, $P < 0.01$.

24 h after transfection, transfection of ERK5 siRNA significantly reduced mitotic index (Fig. 3 C, bottom).

In the experiments described in Fig. 3, HeLa cells were synchronized at early S phase with thymidine 1 d after transfection, well before a considerable amount of transfected ERK5 was expressed (unpublished data) or siRNA reduction of endogenous ERK5 protein occurred. Furthermore, ERK5 activation at G1 and S phases was almost undetectable in HeLa cells. Therefore, data in Fig. 3 (B and C) suggest that ERK5 signaling may regulate mitotic entry and/or progression. To strengthen this conclusion, we designed an experiment to block ERK5 activity from G2 to M phases onward to avoid any potential interference with the G1 and S phases. We took advantage of the fact that adenoviral-mediated gene expression, monitored by GFP expression and Western analysis, occurs 6 h after viral infection (Fig. 3 D). HeLa cells were synchronized in early S phase by a single-thymidine treatment. 2 h after release from thymidine, cells were infected with an adenovirus that expresses both GFP and dnMEK5 (Watson et al., 2001). This allowed expression of dnMEK5 starting from G2 and continuing onward. The dnMEK5 used in this experiment inhibits the signaling of ERK5 but not other related MAPKs (Kato et al., 1997; Cavanaugh et al., 2001; Watson et al., 2001). Expression of the adenoviral dnMEK5 significantly reduced mitotic index in adenovirus-infected cells 12 h after thymidine release (Fig. 3 E). Together, data in Fig. 3 suggest that ERK5 regulates G2–M progression.

ERK5 activates NFκB at G2–M

Activation of ERK5 regulates several downstream targets, including NFκB (Pearson et al., 2001), a transcription factor implicated in cellular proliferation. To determine whether ERK5 activation at G2–M leads to NFκB activation, we transfected HEK293 cells with an NFκB-luciferase reporter to monitor NFκB activity. Cells were also cotransfected with dnERK5 to block endogenous ERK5 signaling. We used HEK293 cells to measure NFκB activities because the basal NFκB activity in HeLa cells is very high (unpublished data). As in HeLa cells, ERK5 phosphorylation was mainly detected in nocodazole-arrested M phase HEK293 cells (unpublished data). The NFκB reporter gene was activated in HEK293 cells after nocodazole treatment or when cells were released from a single-thymidine block for 12 h (Fig. 4 A). Importantly, expression of dnERK5 significantly reduced NFκB-luciferase activity under both conditions. Although the NFκB reporter was only activated 150% 12 h after thymidine release, this stimulation was statistically significant and consistent with the mitotic index of 22% in thymidine-released cells compared with 68% in nocodazole-treated cells. In addition, NFκB-luciferase reporter activities were increased in mitotic cells compared with nonmitotic control cells after the mitotic shake off (Fig. 4 B).

Similar experiments were performed using an NFκB DNA binding ELISA assay. As a positive control, HEK293 cells were transfected with caMEK5 + wtERK5 to activate ERK5. NFκB DNA binding was activated in cells expressing caMEK5 with ERK5 and in cells treated with nocodazole for 12 h (Fig. 4 C). Expression of dnERK5 significantly inhibited NFκB DNA binding activities afforded by caMEK5 expression or nocodazole treatment. Finally, nocodazole treatment also increased the DNA binding activity of NFκB measured by a conventional gel shift assay, and the expression of dnMEK5 prevented this increase (Fig. 4 D). These data suggest that stimulation of ERK5 at G2–M causes activation of NFκB.

ERK5 activates NFκB by causing IκB degradation, a process that is regulated by ribosomal S6 kinase 2 (RSK2)

In resting cells, the p50/p65 heterodimer of NFκB is normally sequestered in the cytoplasm by the inhibitor protein, IκB (Karin et al., 2002). Upon stimulation, IκB is phosphorylated on serine-32 and serine-36 residues. This targets IκB for proteasome-mediated degradation, thereby releasing NFκB and allowing its nuclear translocation and DNA binding (Beg et al., 1992). Data in Fig. 4 demonstrated that ectopic ERK5 activation or M phase arrest by nocodazole treatment increases NFκB binding to DNA,

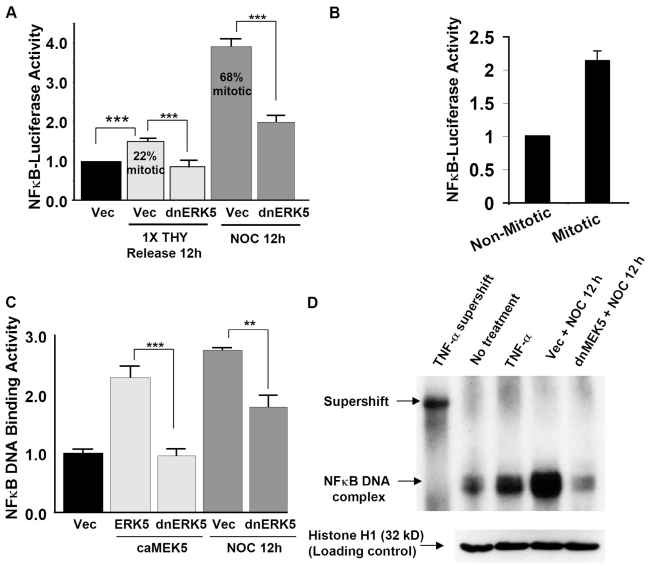

Figure 4. **ERK5 activation at G2–M leads to NFκB stimulation.** (A) NFκB-luciferase activity is increased in HEK293 cells 12 h after thymidine release or after nocodazole (NOC) treatment. HEK293 cells were cotransfected with an NFκB-luciferase reporter and dnERK5 or vector control (Vec) and treated with 2 mM thymidine for 16 h to synchronize at S phase. Luciferase activity was measured 12 h after thymidine release. Alternatively, cells were treated with 0.5 μg/ml nocodazole 36 h after transfection, and reporter gene activity was assayed 12 h later. (B) NFκB-luciferase activity is increased in mitotic cells. HEK293 cells were treated with 2 mM thymidine for 16 h. The thymidine block was released for 8 h, during which cells were transfected with an NFκB-luciferase reporter. The cells were then treated with thymidine again for 16 h. Mitotic cells were gently shaken off the tissue culture dish 9 h after release from the second thymidine block, and NFκB-luciferase activity was measured. Cells that were still attached to the culture dish were used as nonmitotic control cells. The luciferase activity in both A and B was normalized to the cotransfected β-gal. (C) NFκB DNA binding ELISA assay. HEK293 cells were transfected with vector control, caMEK5, wtERK5, or dnERK5 as indicated. NFκB-DNA binding ELISA assay was performed 48 h later. 0.5 μg/ml nocodazole treatment was performed 36 h after transfection. (D) NFκB-DNA binding measured by an electrophoretic mobility shift assay. HeLa cells were transfected with Vec or dnMEK5 and treated with nocodazole for 12 h as in C. The TNFα-treated sample was used as a positive control and subjected to supershift analysis to confirm NFκB-DNA binding specificity. Histone-H1 Western was used as a loading control. Data are presented as means ± SEM. **, $P < 0.01$; ***, $P < 0.001$.

suggesting that NFκB activation may be due to IκB degradation. Indeed, IκB protein levels were reduced in nocodazole-treated HeLa cells, and its degradation was partially blocked by dnERK5 (Fig. 5 A). This suggests that ERK5 regulates the degradation of IκB during G2–M phases of the cell cycle.

Although ERK5 activity is required for NFκB activation, ERK5 does not directly bind to or modulate either IκB or NFκB (unpublished data). This suggests that another kinase may be acting as a mediator between ERK5 and IκB. The most studied IκB kinases are the IKK family of enzymes (Hayden and Ghosh, 2004). We monitored IKK activation at G2 and M phases by Western analysis using an antibody that recognizes phosphorylated and activated IKK (p-IKK). IKK was phosphorylated 3–6 h after release from double-thymidine block (Fig. 5 B), a time when the majority of cells were in S phase and ERK5 was not activated. IKK phosphorylation in S phase is consistent with a role for NFκB in G1–S control. However, IKK was not phosphorylated 9–12 h after thymidine release, when the majority of cells were in G2–M and ERK5 was maximally activated. Furthermore, although ERK5 was activated in a cell population enriched with mitotic cells (Fig. 1 D), IKK phosphorylation was not detectable in this same preparation (Fig. 5 B). These data indicate that IKK does not mediate ERK5 activation of NFκB at G2–M phases of the cell cycle.

RSK1 and RSK2 are downstream targets of the ERK1/2 pathway that can directly phosphorylate IκB, thereby targeting IκB for degradation (Ghoda et al., 1997; Schouten et al., 1997). It has been reported that ERK5 activates RSK2 in NIH 3T3 cells and in neurons (Pearson et al., 2001; Watson et al., 2001). To determine whether RSK1 or RSK2 is activated by ERK5 in our system, HEK293 cells were transfected with caMEK1, which is sufficient to activate endogenous ERK1/2, or with

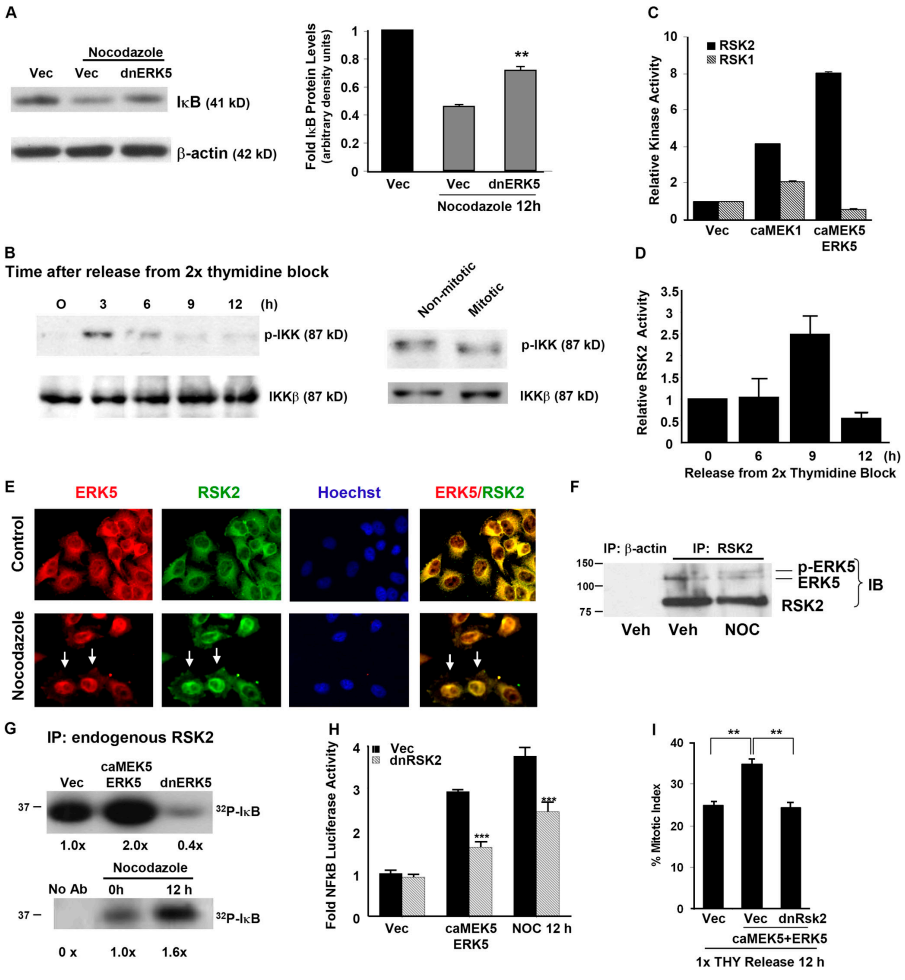

Figure 5. **ERK5-dependent IκB degradation and NFκB activation during G2–M is mediated by RSK2 but not IKK.** (A) The IκB protein is degraded in M phase–arrested cells in an ERK5-dependent manner. HeLa cells were transfected with vector control (Vec) or dnERK5 and treated with 0.5 μg/ml nocodazole for 12 h. IκB protein levels were normalized against β-actin. (B) In contrast to ERK5, IKK is not activated at G2–M or in mitotic cells. HeLa cells were synchronized by a double-thymidine block. The activation of endogenous IKK at various times after thymidine release was analyzed by anti–phospho-IKK Western blotting (left). The protein level for IKK was analyzed by anti-IKK immunoblotting. Alternatively, the same set of lysates prepared from mitotic and nonmitotic cells described in Fig. 1 D were subjected to Western analysis for IKK phosphorylation (right). (C) ERK5 increases the kinase activity of RSK2, but not RSK1, toward a known substrate CREBtide. HEK293 cells were transfected with vector control or caMEK5 + ERK5. Endogenous RSK1 or RSK2 was immunoprecipitated, and their kinase activities were measured by an in vitro kinase assay using CREBtide as a substrate. caMEK1, which activates endogenous ERK1/2, was used as a positive control for both RSK1 and RSK2. (D) RSK2 is activated at G2–M. Endogenous RSK2 was immunoprecipitated from HeLa cells released from a double-thymidine block and its kinase activity measured as in C. (E) 0.5 μg/ml nocodazole treatment for 6 h induces nuclear translocation of ERK5 and RSK2 in HeLa cells. Data were confocal images after immunostaining. Arrows point to two cells with nuclear staining for ERK5 and RSK2. (F) ERK5 and RSK2 interact with each other. HeLa cells were treated with 0.5 μg/ml nocodazole (NOC) or vehicle control (Veh) for 12 h. Endogenous RSK2 was immunoprecipitated (IP) from 300 μg of total cell lysates, and its association with ERK5 was analyzed by anti-ERK5 Western blotting (IB). Anti-RSK2 Western blotting was performed on the same blot as a loading control of the immunoprecipitated material. Immunoprecipitation using an unrelated antibody (anti–β-actin) was used as a negative control for the coimmunoprecipitation. (G) Both constitutive ERK5 activation and nocodazole treatment increase RSK2 phosphorylation of IκB. HEK293 cells were transfected with caMEK5 + ERK5, dnERK5, or Vec (top). Alternatively, HEK293 cells were treated with nocodazole for 0 or 12 h (bottom). Endogenous RSK2 was immunoprecipitated and its kinase activity toward IκB measured by an in vitro kinase assay using human recombinant IκB protein as a substrate. (H) NFκB-dependent transcription, either induced by constitutive ERK5 activation or by nocodazole treatment, requires RSK2 activity. HEK293 cells were transfected with a NFκB-luciferase reporter gene together with dnRSK2 or vector control. Cells were also cotransfected with caMEK5 + ERK5 or vector control or treated with nocodazole to stimulate NFκB. (I) Expression of dnRSK2 blocks mitotic entry induced by constitutive activation of ERK5. HeLa cells were transfected with various plasmid DNA as indicated. Cells were also cotransfected with EGFP to identify transfected cells. Cells were treated 24 h later with thymidine for 16 h. Mitotic index in transfected cell population (GFP^+) was quantified 12 h after thymidine release. Data are presented as means ± SEM. **, $P < 0.01$; ***, $P < 0.001$.

caMEK5 + wtERK5 to activate ERK5 signaling. Constitutive activation of the ERK1/2 pathways increased the activity of both RSK1 and RSK2, whereas constitutive activation of ERK5 only activated RSK2 (Fig. 5 C). These data suggest that RSK2, but not RSK1, may mediate ERK5 activation of NFκB.

To determine whether RSK2 is activated at G2 and M phases, the kinase activity of endogenous RSK2 was measured in HeLa cells synchronized by double-thymidine block. Like ERK5, RSK2 was activated 9 h after thymidine release, when the majority of cells were at G2–M (Fig. 5 D). RSK2 was also activated in the cell population enriched with mitotic cells (unpublished data). Furthermore, RSK2 colocalized with ERK5 in nocodazole-treated HeLa cells (Fig. 5 E). In control cells, both RSK2 and ERK5 were localized in the cytosol. Nocodazole treatment for 6 h induced nuclear translocation of both proteins in some cells. Moreover, immunoprecipitation of endogenous RSK2 isolated from nocodazole-treated HeLa cells pulled down both phospho-ERK5 and nonphospho-ERK5 protein (Fig. 5 F), suggesting a physical interaction between ERK5 and RSK2. This is consistent with a recent report documenting an interaction between ERK5 and RSK2 (Ranganathan et al., 2006).

The kinase activity of endogenous RSK2 toward IκB was directly measured by an in vitro kinase assay. RSK2 phosphorylation of IκB protein increased 2- or 1.6-fold in HeLa cells expressing caMEK5 + ERK5 or in nocodazole-treated HeLa cells, respectively (Fig. 5 G). Expression of dnERK5 reduced basal RSK2 kinase activity toward IκB by 60%. Furthermore, expression of dnRSK2 abrogated NFκB activation induced by nocodazole or by expression of caMEK5 + ERK5 (Fig. 5 H).

To test the functional consequence of RSK2 activation by ERK5 in G2–M regulation, HeLa cells were transfected and treated as in Fig. 3 B. A dnRSK2 was transfected to inhibit RSK2 signaling. As shown in Fig. 3 B, ectopic activation of ERK5 increased the mitotic index 12 h after thymidine release. This increase was blocked by coexpression of dnRSK2 (Fig. 5 I). Together, these data suggest that RSK2 is activated downstream from ERK5 at G2–M phases of the cell cycle and that ERK5 activates NFκB via RSK2-dependent IκB phosphorylation and degradation.

NFκB regulates mitotic entry

The specific NFκB inhibitors SN50 and helenalin were used to determine whether NFκB-dependent transcription is necessary for G2–M progression. As a positive control, we confirmed that SN50 and helenalin block NFκB-stimulated transcription after TNFα treatment (unpublished data). SN50 and helenalin were added to HeLa cells 8 h after release from a single-thymidine block (Fig. 6) or 6 h after a double-thymidine block (Fig. 7) to interfere with the G2–M, but not G1–S, function of NFκB. Both SN50 and helenalin greatly decreased the mitotic index 12 h after release from a single-thymidine block (Fig. 6, A and B).

We determined whether there is a critical time when blocking NFκB signaling inhibits mitosis. SN50 was added 8 or 10 h after release from a single-thymidine block, times corresponding to the beginning and midpeak of appearance of mitotic cells, respectively. Interestingly, addition of SN50 8 h, but not 10 h, after thymidine release reduced the mitotic index (Fig. 6 C). Similar results were obtained when actinomycin D was used to block general transcription (unpublished data). These data suggest that NFκB-mediated transcription regulates G2–M progression.

The kinetics for the effect of helenalin on mitosis were also examined. HeLa cells were synchronized with a double-thymidine block and treated with helenalin 6 h after thymidine release to inhibit NFκB from G2 phase onward. Helenalin did not affect the rate of appearance of cells harboring 4n DNA 9 h after thymidine release (Fig. 7 A), suggesting that DNA synthesis and S phase completion were unaffected. However, there was a delay in the reappearance of 2n DNA–containing cells (G0–G1) and in the disappearance of 4n DNA–containing cells (G2–M) 9–14 h after thymidine release, suggesting that cells were staying at G2–M longer. This could have resulted from a delay in mitotic entry, meaning cells spent more time in G2, or a delay in mitotic exit in which cells stayed in M phase longer. Because the majority of the cells still harbored 4n DNA and were in G2 or M phases of the cell cycle 10 h after release from a single-thymidine block (Fig. 2 B), the fact that treatment with SN50 at this time did not affect the mitotic index

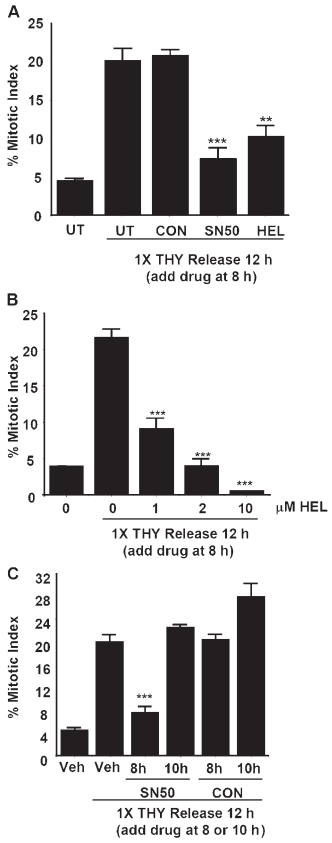

Figure 6. **Effect of pharmacological inhibition of NFκB on mitosis.** HeLa cells were released from a single-thymidine block. (A) Addition of SN50 or helenalin (HEL) at the start of G2 reduces mitotic index monitored 12 h after thymidine release. HeLa cells were left untreated (UT) or treated with 18 μM SN50 peptide, control peptide (CON), or 1 μM helenalin 8 h after thymidine release. (B) Dose response of helenalin inhibition of mitosis. (C) Addition of SN50 8 h, but not 10 h, after thymidine release reduces mitotic index. Veh, vehicle control. Data are presented as means ± SEM. **, $P < 0.01$; ***, $P < 0.001$.

(Fig. 6 C) favors the former explanation. To more clearly distinguish between these two possibilities, taxol or nocodazole was included to block mitotic exit and trap mitotic cells so any defects in mitotic entry can be detected unambiguously. Helenalin treatment in the presence of taxol or nocodazole delayed accumulation of mitotic cells (Fig. 7, B and C), suggesting that NFκB activity is required for mitotic entry.

In addition to the pharmacological inhibitors, we used an adenovirus encoding a nondegradable IκB super repressor (SR) mutant protein to specifically block NFκB activation (Wang et al., 1996). When infected 2 h after release from a single-thymidine block, the adenoviral IκB SR was abundantly expressed 6 h later, when cells enter mitosis (Fig. 7 D). Expression of IκB SR from G2 phase onward delayed the appearance of mitotic cells after HeLa cells were released from a double-thymidine block (Fig. 7 E). This reduction in mitotic index persisted when mitotic exit was blocked by taxol. Similar to treatment with helenalin, expression of IκB SR did not affect the rate of initial appearance of cells harboring 4n DNA between 6 and 9 h (Fig. 7 F), suggesting that DNA synthesis and S phase completion were unaffected. However, the disappearance of 4n DNA–containing cells and reappearance of 2n DNA–containing cells slowed down. Together, data in Fig. 7 demonstrate that blocking NFκB signaling delays mitotic entry.

ERK5 promotion of G2–M transition requires NFκB

To establish a direct link between ERK5 and NFκB at G2–M progression, HeLa cells were transfected with caMEK5 + wtERK5. 1 d later, cells were synchronized at S phase by a single-thymidine block. 2 h after thymidine release, cells were infected with the IκB SR adenovirus to selectively block NFκB signaling at G2–M. Expression of this IκB SR at G2–M greatly reduced the mitotic index (Fig. 8 A). Similar results were obtained when SN50 or helenalin was used to inhibit NFκB signaling at G2–M (Fig. 8 B). This supports the hypothesis that ERK5 activation of NFκB is critical for G2–M progression during the cell cycle.

NFκB regulates the transcription of genes critical for mitotic entry

To identify target genes of the ERK5–NFκB pathway that regulate G2–M transition, quantitative RT-PCR was performed to investigate the effect of blocking NFκB on the transcription of several genes known to be critical for mitotic entry. These include cyclin B1 and B2 (Pines and Hunter, 1990), polo-like kinase-1 (Plk-1; Barr et al., 2004), and protein phosphatase cdc25B (Nilsson and Hoffmann, 2000). HeLa cells were synchronized by a double-thymidine block and then infected with control or IκB SR adenovirus at the time of thymidine release to inhibit NFκB from G2 phase onward. The transcripts of cyclin B1, cyclin B2, Plk-1, and cdc25B were increased 9 h after thymidine release (Fig. 9, A–D). Up-regulation of these transcripts was inhibited by IκB SR. The incomplete suppression of transcription suggests that other factors may also contribute to the transcriptional regulation of these genes.

We also transfected cells with a cyclin B1-CAT reporter construct to monitor transcription initiated from the cyclin B1 promoter. Nocodazole treatment stimulated cyclin B1-CAT activity, which is inhibited by coexpression of dnERK5 (Fig. 9 E). Collectively, these data suggest that the ERK5–NFκB signaling pathway regulates expression of several genes key to the control of G2–M transition.

ERK5-NFκB signaling is required for G2-M progression in cultured primary human cells

We used human artery smooth muscle cells (hSMCs) and human foreskin fibroblast (HFF) cells to investigate whether the ERK5–NFκB signal transduction system is also required for G2–M progression in nonimmortalized, nontransformed, primary human cells.

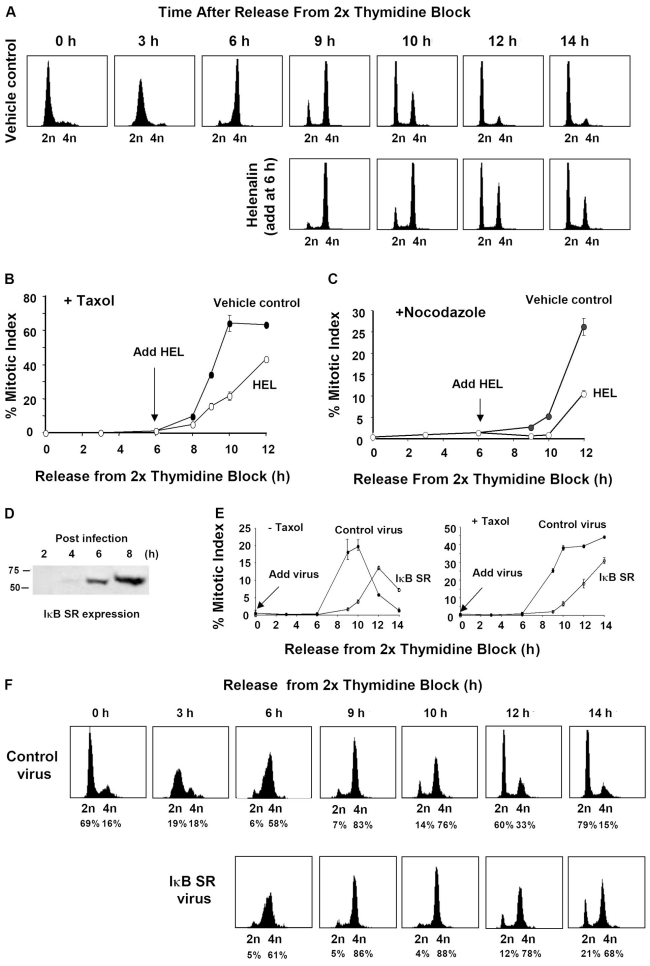

Figure 7. **Inhibition of NFκB from G2–M onwards delays mitotic entry.** HeLa cells were released from a double-thymidine block. (A). FACS analysis of the cell cycle. 2 μM helenalin or vehicle control was added 6 h after thymidine release to inhibit NFκB from G2 onward. (B) Addition of helenalin (HEL) at the start of G2 inhibits mitotic entry in the presence of 1 μM taxol. (C) Addition of helenalin at the start of G2 inhibits mitotic entry in the presence of 0.5 μg/ml nocodazole. (D) Time course of adenovirus-mediated expression of IκB SR. (E) Expression of IκB SR from G2 onward delays mitotic entry. Double-thymidine block–synchronized HeLa cells were infected with IκB SR or control viruses at the time of thymidine release. Cells were incubated in medium ± 1 μM taxol. (F) FACS analysis of the cell cycle after IκB SR expression. HeLa cells were synchronized and infected with viruses as in E. Data are presented as means ± SEM.

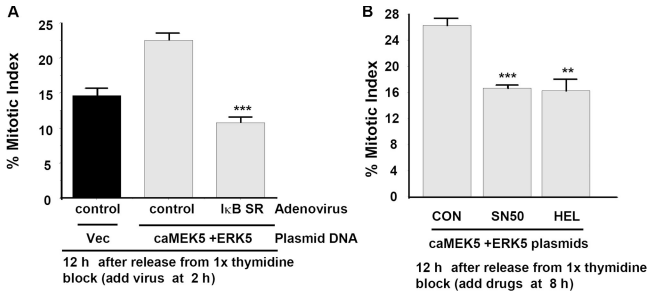

Figure 8. **NFκB is required for ERK5 to promote G2–M progression.** HeLa cells were transiently transfected with a vector control (Vec) or caMEK5 + ERK5 to activate ERK5 signaling. 1 d after transfection, cells were arrested at S phase with a single-thymidine block. (A) Cells were infected with IκB SR or a control adenovirus 2 h after thymidine release. (B) SN50, the control peptide (CON), or 1 μM helenalin (HEL) was added 8 h after thymidine release. Mitotic index in transfected cells was determined 12 h after thymidine release. Data are presented as means ± SEM. **, $P < 0.01$; ***, $P < 0.001$.

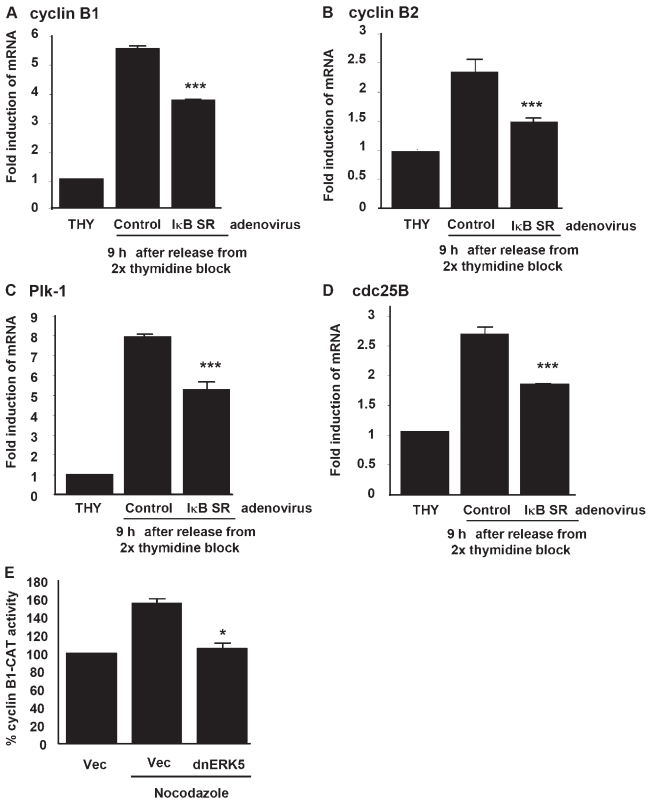

Figure 9. **NFκB regulates transcription of G2–M specific genes.** (A–D) Transcription of cyclin B1, cyclin B2, Plk-1, and cdc25B at G2–M is inhibited by IκB SR expression. HeLa cells were infected with control or IκB SR adenoviruses at the time of release from a double-thymidine block. Non–virus infected, double-thymidine–blocked cells were used as a control. Total RNA was prepared 9 h after thymidine release for quantitative RT-PCR. (E) Nocodazole stimulates cyclin B promoter activity in an ERK5-dependent manner. HEK293 cells were cotransfected with a cyclin B1-CAT reporter gene and dnERK5 or vector control (Vec). 36 h later, cells were treated with nocodazole for 12 h. Error bars indicate SD. *, $P < 0.05$; ***, $P < 0.001$.

ERK5 was activated in M phase–arrested hSMCs and HFF cells, an activation manifested as a phosphorylation shift of ERK5 (p-ERK5) in nocodazole-treated cells (M; Fig. 10, A and B). Significantly, expression of adenoviral dnMEK5 or IκB SR reduced the mitotic index in hSMC (Fig. 10 C). Inhibition of NFκB activity by SN50 or helenalin significantly reduced mitotic index in HFF cells (Fig. 10 D). These results implicate a role for the ERK5–NFκB signal pathway in G2–M progression during the cell cycle of primary human cells.

Discussion

Although regulation of the G1 phase has been extensively investigated, much less is known about regulation of the G2–M phase transition. Besides a requirement for cyclin B and cdc2 activation, few other genes or signaling molecules have been identified for the control of the G2–M transition. Here, we discovered that ERK5 is activated at G2–M and is critical for the G2–M transition and timely mitotic entry. This function requires ERK5 activation of NFκB through RSK2. Furthermore, NFκB regulates the expression of several genes essential for mitosis, including cyclin B1, cyclin B2, Plk-1, and cdc25B. We also observed the activation and requirement of the ERK5–NFκB pathway for the G2–M progression in primary cultured human cells. These data suggest a novel function for the ERK5–NFκB pathway in regulation of the G2–M transition in both primary and transformed cells.

To investigate the functional significance of ERK5 activation at G2–M, we performed several types of experiments to examine the effects of blocking or stimulating ERK5 activity on mitosis. Constitutive activation of the ERK5 pathway was sufficient to increase the mitotic index in an asynchronous cell population, whereas blocking ERK5 activity with dnERK5 or siRNA reduced mitotic index in S phase–synchronized HeLa cells. Most important, expression of adenoviral dnMEK5 from G2 onward, which eliminates potential interference of ERK5 signaling at G1 or S phase of the cell cycle, reduced mitotic index. These data are the first report of a causal relationship between ERK5 activation and G2–M progression.

Although ERK5 had been implicated in cellular proliferation, the underlying mechanisms were not defined. It has been reported that ERK5 regulates the G1–S transition of the cell cycle; however, evidence supporting this hypothesis is controversial. For example, some reports showed that dnMEK5 inhibition of ERK5 in NIH 3T3 cells blocks EGF stimulation of thymidine incorporation (Kato et al., 1998) and ERK5 may activate cyclin D1 expression (Mulloy et al., 2003). In contrast, although MEK5 knockout mice have a phenotype similar to the ERK5-null mice, mouse embryonic fibroblast cells derived from $MEK5^{-/-}$ mice do not exhibit a defect in G1–S (Wang et al., 2005). Our data demonstrate that ERK5 phosphorylation is barely detectable in HeLa cells arrested at G1 or S phase when HeLa cells are released from a thymidine block. This is consistent with the report by Wang et al. (2005) arguing against a role for ERK5 in G1–S regulation. Thus, ERK5 may regulate cellular proliferation primarily through its action at the G2–M phases of the cell cycle.

What are the downstream targets that mediate ERK5 regulation of the G2–M transition? Our data showed that NFκB is activated when cells were arrested at the start of M phase by

nocodazole treatment, 12 h after thymidine release, or in mitotic shake-off cells. Furthermore, NFκB activation in G2–M requires ERK5 activity. Inhibition of NFκB starting from G2 phase onward, achieved by treatment with helenalin or SN50, or by expression of adenoviral IκB SR, reduced the mitotic index. The delay in the rate of appearance of mitotic cells was also observed when mitotic exit was blocked by taxol or nocodazole, suggesting a pivotal role for NFκB in timely mitotic entry. In addition, stimulation of mitosis in cells transfected with caMEK5 + ERK5 was suppressed by inhibiting NFκB from G2 onward, demonstrating a direct link between ERK5 and NFκB at G2–M. These data suggest a novel function for the ERK5–NFκB pathway in the regulation of G2–M transition.

The transition from G2 to M phase requires activation of the cyclin B–cyclin-dependent kinase 1 (CDK1, also known as cdc2) complex (Nurse, 2000). The cyclic activation of this complex at G2–M is stimulated by dephosphorylation of CDK1 and increased expression of cyclin B. This process is regulated by several G2–M kinases and phosphatases, including cdc25 and Plk (Nilsson and Hoffmann, 2000; Barr et al., 2004). The activity and expression of cdc25 and Plk are also regulated in a cell cycle–dependent manner. Although it is clear that many of these G2–M regulators are controlled transcriptionally in a cell cycle–specific manner, mechanisms underlying their transcriptional regulation are not well defined. Recently, it was reported that the forkhead family of transcription factors, including FOXM1 and FoxO, play a critical role in the expression of genes important for mitotic entry and exit (Alvarez et al., 2001; Laoukili et al., 2005). In this study, we discovered that blocking NFκB signaling at G2–M inhibits transcription of cyclin B1, cyclin B2, Plk-1, and cdc25, suggesting an important role for NFκB in the transcriptional regulation of these genes. These findings provide new insights concerning transcriptional mechanisms governing G2–M progression of the cell cycle. Although NFκB has been implicated in cell proliferation and many forms of human cancer, NFκB activity has only been implicated in regulation of the G1–S phases of the cell cycle through induction of the G1 cyclin, cyclin D (Guttridge et al., 1999; Hinz et al., 1999). Our study identifies a new function for NFκB in the regulation of G2–M transition.

It has been reported that forced activation of ERK5 stimulates NFκB reporter gene expression; however, the mechanism by which ERK5 activates NFκB was not elucidated (Pearson et al., 2001). NFκB-mediated transcription can be stimulated by increased DNA binding or by an NFκB phosphorylation that enhances the recruitment of transcriptional coactivators (Wang et al., 2000). However, we found that ERK5 does not directly stimulate Gal-4–NFκB–mediated transcription (unpublished data). Instead, IκB protein was degraded and NFκB DNA binding activity increased in M phase–arrested cells; both processes required ERK5 activity. These data support the hypothesis that NFκB activation at G2–M is mediated by ERK5 stimulation of IκB degradation and subsequent NFκB binding to DNA.

Previous studies showed that NFκB activation by nocodazole requires IKK in some cells and that this promotes cell survival after mitotic cell cycle arrest (Mistry et al., 2004). Surprisingly, IKK was not active at G2–M, when HeLa cells

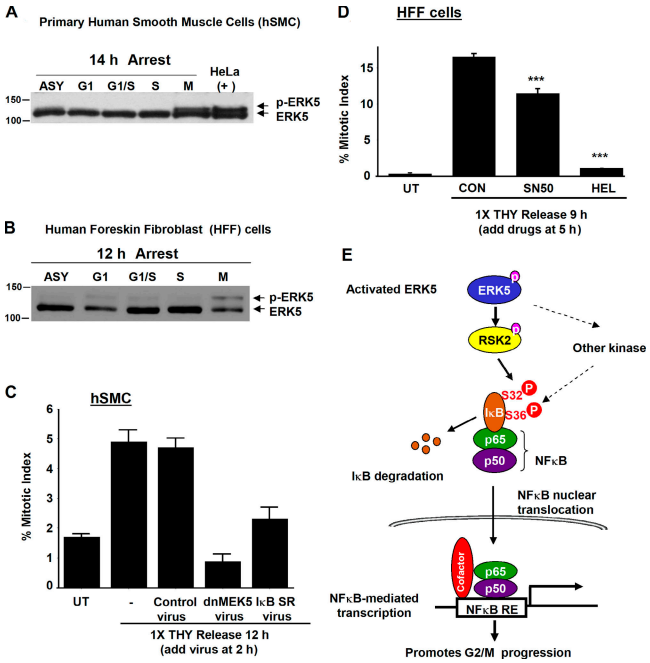

Figure 10. **ERK5–NFκB signaling is required for G2–M progression in cultured primary human cells.** (A and B) ERK5 Western analysis demonstrating that ERK5 is activated in primary hSMCs (A) and HFF cells (B) arrested with nocodazole at M phase. (C) Inhibition of ERK5 or NFκB signaling reduces mitotic index in hSMCs. Cells were synchronized at S phase by a single-thymidine block and infected with dnMEK5, IκB SR, or control adenoviruses 2 h after thymidine release. Mitotic index was scored 12 h after thymidine release (i.e., 10 h after infection). Minus sign indicates no virus. UT, untreated. (D) Inhibition of NFκB reduces mitotic index in HFF cells. Cells were synchronized at S phase by a single-thymidine block. To inhibit NFκB signaling starting from G2, cells were treated with 18 μM SN50, 1 μM helenalin, or control peptide (CON) 5 h after thymidine release. Mitotic index was determined 9 h after thymidine release. (E) Hypothesis model for ERK5 regulation of G2–M progression. Based on data presented in this study, we propose that ERK5 activation of RSK2 at G2–M promotes IκB phosphorylation and degradation. This leads to NFκB nuclear translocation and induction of NFκB target genes that are required for the G2–M progression. Data are presented as means ± SEM. ***, $P < 0.001$.

were released from a thymidine block, or in a cell population enriched for mitotic cells. Thus, although IKK may counteract nocodazole-induced apoptosis by acting as an IκB kinase in some cells, it does not mediate ERK5 activation of NFκB during G2–M progression of the cell cycle.

RSK1 and RSK2 both phosphorylate IκB (Ghoda et al., 1997; Schouten et al., 1997). However, ERK5 stimulated the activity of RSK2, but not RSK1. Furthermore, RSK2 was activated at G2–M and physically associated with ERK5. Constitutive activation of ERK5 promoted RSK2 phosphorylation of IκB, whereas blocking ERK5 reduced the kinase activity of RSK2 toward IκB. Moreover, RSK2 activity was required for NFκB activation induced by ERK5 or M phase arrest. Expression of dnRSK2 blocked mitotic entry of HeLa cells induced by ectopic ERK5 activation. These results suggest that RSK2 is necessary for ERK5-induced degradation of IκB at G2–M. However, RSK2 phosphorylates IκB on S32, but not S36, which is necessary but not sufficient for IκB degradation (Beg et al., 1992; Liu et al., 1996). Thus, it is likely that, in addition to RSK2, ERK5-mediated phosphorylation of IκB may require

another, unidentified kinase that mediates ERK5 phosphorylation of IκB at S36.

We were unable to achieve complete inhibition of mitotic entry by blocking ERK5, RSK2, or NFκB, possibly because none of the experimental approaches completely blocked the signaling events, or there may be additional pathways involved. Furthermore, because inhibition of NFκB delays but does not completely halt mitotic progression (Fig. 7), it is possible that the ERK5–RSK2–NFκB signaling pathway plays a regulatory rather than obligatory role in the G2–M cell cycle control as exemplified by FoxM1 (Laoukili et al., 2005).

In summary, we propose that ERK5 is activated at G2–M and that it stimulates downstream kinases, including RSK2 kinase (Fig. 10 E). RSK2 phosphorylates IκB, targeting it for degradation, thereby releasing NFκB from IκB. Subsequently, NFκB translocates to the nucleus and activates expression of target genes that are required for the G2–M progression. Our studies identify an unexpected and novel role for the ERK5–NFκB pathway in G2–M regulation.

Materials and methods

Materials

HEK293 and HeLa cells were purchased from American Type Culture Collection. HEK293 cells were used for reporter gene assays and NFκB DNA binding assays because the basal NFκB activity is very high in HeLa cells. However, for flow cytometry and immunocytochemistry, HeLa cells were routinely used because HEK293 cells grow in clusters and clumps, making it difficult to analyze by these assays. Primary hSMCs were provided by B. Askari and K. Bornfeldt (University of Washington, Seattle, WA; Renard et al., 2003). HFF cells were provided by A. Minella and B. Clurman (Fred Hutchinson Cancer Research Center, Seattle, WA; Minella et al., 2002). A commercial siRNA to human ERK5 and control nonsilencing RNA (NS) were obtained from Ambion. The following plasmids were obtained from J.D. Lee (The Scripps Research Institute, La Jolla, CA): wt and dnERK5 and HA-tagged caMEK5 (Kato et al., 1997). The flag-tagged dnRSK2 construct was a gift from S. Impey (Oregon Health Sciences University, Portland, OR). The cyclin B1-CAT (pB1-CAT) reporter plasmid was provided by G. Piaggio and C. Gaetano (CRS-IRE, Rome, Italy; Piaggio et al., 1995). The dnMEK5 adenovirus was a gift from R. Segal (Dana Farber Cancer Institute, Boston, MA). The NFκB-luciferase reporter and IκB SR adenovirus have been described previously (Wang et al., 1996). The polyclonal antibody to ERK5 was generated in our laboratory (Cavanaugh et al., 2001). The following antibodies were obtained commercially: anti-RSK2, anti–phospho-histone H3 (Ser10), and anti–phospho-MPM-2 (Upstate Biotechnology), anti–phospho-IκB Ser32 or Ser36 (Calbiochem), anti–phospho-IKK Ser180/181 and anti-IκB (Cell Signaling Technologies), anti-MEK5 antibody (Santa Cruz Biotechnology, Inc.), and anti-ERK1/2 antibody (Promega). Cell-permeable NFκB inhibitor SN50 and control peptides, helenalin, thymidine, nocodazole, taxol, and aphidicolin were purchased from Calbiochem. Hoechst 33342 was obtained from Sigma-Aldrich. Myelin basic protein (MBP) was purchased from Upstate Biotechnology.

Transient DNA/siRNA transfection

HeLa or HEK293 cells (10^6 cells/60-mm dish) were transiently transfected with plasmid DNA by Fugene 6 (Roche). siRNA was transiently transfected using Oligofectamine (Invitrogen).

Cell cycle synchronization

HEK293, HeLa, and HFF cells were arrested in different cell cycle phases as follows: serum withdrawal for 14 h followed by addition of serum for 1 h (G1), 1 μg/ml aphidicolin (G1–S; 12 h), 2 mM thymidine (S; 14–16 h), or 0.5 μg/ml nocodazole (M; 12 h). Cell cycle arrest was confirmed by flow cytometry analysis. Primary hSMCs were arrested using similar drug treatments for 14 h. Initially, cells were synchronized at early S phase by a single-thymidine block, in which cells were treated with 2 mM thymidine for 15 h, released from the block by washing cells in PBS three times, and grown in complete medium for the indicated times up to 12 h. In later experiments, a double-thymidine block was used to obtain better synchrony. Cells were treated with 2 mM thymidine for 16 h and released for 8 h, followed by an additional 16-h thymidine block and release. The cells were then washed three times with PBS and released into complete medium. To examine the effect of adenoviral gene expression or drug treatment on mitosis, NFκB inhibitors and adenoviruses were added at the indicated times after final thymidine release.

Reporter gene assays

HEK293 cells were transfected using Fugene 6 by the manufacturer's instructions. In brief, 0.15×10^6 cells were plated onto each well of a 24-well plate coated with poly-D-lysine (Sigma-Aldrich). After 24 h, cells were transfected with the appropriate reporter genes (0.36 μg/well NFκB-luciferase plus 0.05 μg/well EF1α-lacZ plasmid DNA). Where indicated, cells were cotransfected with 0.16 μg/well dnERK5. Cells were treated 48 h after transfection, and luciferase and β-galactosidase activities were measured. For the cyclin B1-CAT reporter assay, HEK293 cells were cotransfected with a plasmid encoding dnERK5, the reporter plasmid pB1-CAT, and an EF1α-lacZ plasmid as an internal control. Cell lysates were harvested 48 h after transfection, and CAT activity was assayed in whole-cell extracts as described previously (Piaggio et al., 1995). The reporter gene luciferase or CAT activities were normalized to β-galactosidase activity and expressed as the fold induction relative to control.

NFκB DNA binding assay (assay for p50–p65 DNA binding)

Nuclear fractions were prepared from cell lysates of HEK293 cells using the NucBuster Protein Extraction kit (Novagen) per the manufacturer's instructions. Nuclear NFκB DNA binding activity (the p50–p65 complex) was then quantitated by the NFκB Transcription Factor Assay ELISA kit (Chemicon International) per the manufacturer's instructions. The DNA binding activity of NFκB was also measured by an electrophoretic mobility shift assay (gel shift) as described previously (Wang et al., 1996).

Cell cycle analysis

Except where specified, mitotic cells were scored by nuclear condensation in conjunction with positive staining for p-MPM-2, a mitotic marker. In Fig. 3 A, p-histone H3 was used as another mitotic marker in addition to p-MPM-2. Alternatively, HeLa cells in G1 (2n DNA) or G2–M (4n DNA) were quantitated by flow cytometry analysis (FACS). In brief, cells were trypsinized, resuspended in ice-cold 70% ethanol, and fixed at 4°C for 30 min. Cells were then resuspended in propidium iodide staining buffer containing 200 μg/ml RNase and 2% FBS in 1× PBS and incubated at 4°C for 3 h. Cells were then resuspended in PBS/2% FBS with an 18-gauge needle and analyzed by FACScan analyzer (Becton Dickinson) equipped with a 518-nm laser.

In vitro kinase assays

Cell lysates were prepared from HeLa cells as described previously (Xia et al., 1995). Equal amounts of protein lysates (350 μg) were used for each kinase assay. The kinase activities for ERK5 or MEK5 were measured using immunoprecipitation-coupled in vitro kinase assays using recombinant GST-MEF2C or MBP as substrates, respectively (Cavanaugh et al., 2001; Wang et al., 2006). To measure endogenous RSK2 activity, cell lysates were immunoprecipitated with a polyclonal anti-RSK2 antibody. In brief, 5 μg anti-RSK2 antibody was incubated with 50 μl protein A–Sepharose beads overnight at 4°C. The beads were washed once with lysis buffer and then incubated with cell lysates for 3 h at 4°C. RSK2 kinase activity in the immune precipitates was then quantitated by evaluating the incorporation of [^{32}P]ATP into either 0.1 mM CREBtide (Sigma-Aldrich; Impey et al., 1998) or 1 μg of a recombinant human IκB protein (BIOMOL Research Laboratories, Inc.).

Quantitative RT-PCR

Total RNA was isolated using RNeasy Miniprep kit (QIAGEN). To remove trace genomic DNA, DNA-free (Ambion) treatment was performed on samples. Total RNA was quantitated on the Mx4000 Multiplex QPCR System (Stratagene) using the RiboGreen RNA Quantitation kit (Invitrogen). Quantitative RT-PCR was performed in a single reaction on an Mx4000 Multiplex QPCR System using 20 ng of total RNA. The RT-PCR reactions were performed in triplicates in a 20-μl reaction using SYBR Green PCR Master Mix (Applied Biosystems; 10 μl 2× Master Mix, 400 nM each primer, 5 U MultiScribe RT, and 8 U RNase inhibitor). The cycling conditions were 48°C for 30 min and 95°C for 10 min, followed by 40 cycles of 95°C for 15 s and 60°C for 1 min. After each assay, a dissociation curve was run to confirm specificity of all PCR amplicons. Resulting C_t values were converted to nanograms, normalized to total RNA, and expressed as the mean

of triplicate samples ± SD. Pooled sample total RNA was used for standard curves as 1:2 serial dilutions. The standard curves showed reaction efficiencies as follows: hcdc25B, 102.6% and $R^2 = 0.999$; hPLK1, 102.5% and $R^2 = 0.998$; hCCNB1, 100.6% and $R^2 = 0.998$; and hCCNB2, 101.3% and $R^2 = 0.998$. PCR primers were designed using Primer Express 2.0 software (Applied Biosystems) and synthesized by Operon. The sequences were as follows: hcdc25B, forward, CCCTATGGACCCCCACATG, and reverse, ATGGCAAACTGCTCGTTTCG; hPlk1, forward, GAGCGTGACGGCACTGAGT, and reverse, AAGGAGGGTGATCTTCTTCATCAA; hcyclinB1, forward, GAAATGTACCCTCCAGAAATTGGT, and reverse, CCATCTGTCTGATTTGGTGCTTAG; hcyclinB2, forward, TGTCAACAAACAACTGAAACCTACTG, and reverse, CCTCAGGTGTGGGAGAAGGA.

Microscopy

For Fig. 3 D, images were collected with an inverted fluorescence microscope (Leitz DMIRB; Leica) using a 40× objective lens (Leitz; Leica). MagnaFire digital microscope camera and MagnaFire software (Optronics, Inc.) were used for system control and image processing. For Fig. 1 B and Fig. 5 E, images were taken by a Marianas imaging system (Intelligent Imaging Innovations, Inc.) incorporating a microscope (Axiovert 200M; Carl Zeiss MicroImaging, Inc.) with an X,Y motorized stage, shuttered 175 W xenon lamp coupled with a liquid light guide, a digital camera (CoolSNAP HQ; Roper Scientific), and 40× objective lens (Axiovert; Carl Zeiss MicroImaging, Inc.). Slidebook software package was used for system control and image processing.

Statistical analysis

Results were from three or more independent experiments. Data are presented as means ± SEM for all except in Fig. 9, in which error bars are SD. We used two-tailed *t* test assuming equal variance for statistical analysis of the data. *, $P < 0.05$; **, $P < 0.01$; ***, $P < 0.001$.

We thank Dr. R. Segal for providing the dnMEK5 adenovirus, Drs. B. Askari and K. Bornfeldt for the hSMCs, Drs. A. Minella and B. Clurman for HFF cells, and Mei Xu for technical assistance.

This work was supported by grants from the National Institute on Aging (Z. Xia; AG19193), the National Institute of Dental and Craniofacial Research (DE015973), and the National Cancer Institute (C.-Y. Wang; CA100849).

Submitted: 27 September 2006
Accepted: 21 March 2007

References

Alvarez, B., A.C. Martinez, B.M. Burgering, and A.C. Carrera. 2001. Forkhead transcription factors contribute to execution of the mitotic programme in mammals. *Nature.* 413:744–747.

Barr, F.A., H.H. Sillje, and E.A. Nigg. 2004. Polo-like kinases and the orchestration of cell division. *Nat. Rev. Mol. Cell Biol.* 5:429–440.

Beg, A.A., S.M. Ruben, R.I. Scheinman, S. Haskill, C.A. Rosen, and A.S. Baldwin Jr. 1992. I kappa B interacts with the nuclear localization sequences of the subunits of NF-kappa B: a mechanism for cytoplasmic retention. *Genes Dev.* 6:1899–1913.

Cavanaugh, J.E., J. Ham, M. Hetman, S. Poser, C. Yan, and Z. Xia. 2001. Differential regulation of mitogen-activated protein kinases ERK1/2 and ERK5 by neurotrophins, neuronal activity, and cAMP in neurons. *J. Neurosci.* 21:434–443.

English, J.M., C.A. Vanderbilt, S. Xu, S. Marcus, and M.H. Cobb. 1995. Isolation of MEK5 and differential expression of alternatively spliced forms. *J. Biol. Chem.* 270:28897–28902.

Esparis-Ogando, A., E. Diaz-Rodriguez, J.C. Montero, L. Yuste, P. Crespo, and A. Pandiella. 2002. Erk5 participates in neuregulin signal transduction and is constitutively active in breast cancer cells overexpressing ErbB2. *Mol. Cell. Biol.* 22:270–285.

Finco, T.S., J.K. Westwick, J.L. Norris, A.A. Beg, C.J. Der, and A.S. Baldwin Jr. 1997. Oncogenic Ha-Ras-induced signaling activates NF-kappaB transcriptional activity, which is required for cellular transformation. *J. Biol. Chem.* 272:24113–24116.

Ghoda, L., X. Lin, and W.C. Greene. 1997. The 90-kDa ribosomal S6 kinase (pp90rsk) phosphorylates the N-terminal regulatory domain of IkappaBalpha and stimulates its degradation in vitro. *J. Biol. Chem.* 272:21281–21288.

Guttridge, D.C., C. Albanese, J.Y. Reuther, R.G. Pestell, and A.S. Baldwin Jr. 1999. NF-kappaB controls cell growth and differentiation through transcriptional regulation of cyclin D1. *Mol. Cell. Biol.* 19:5785–5799.

Hayashi, M., and J.D. Lee. 2004. Role of the BMK1/ERK5 signaling pathway: lessons from knockout mice. *J. Mol. Med.* 82:800–808.

Hayden, M.S., and S. Ghosh. 2004. Signaling to NF-kappaB. *Genes Dev.* 18:2195–2224.

Hinz, M., D. Krappmann, A. Eichten, A. Heder, C. Scheidereit, and M. Strauss. 1999. NF-kappaB function in growth control: regulation of cyclin D1 expression and G0/G1-to-S-phase transition. *Mol. Cell. Biol.* 19:2690–2698.

Impey, S., D.M. Smith, K. Obrietan, R. Donahue, C. Wade, and D.R. Storm. 1998. Stimulation of cAMP response element (CRE)-mediated transcription during contextual learning. *Nat. Neurosci.* 1:595–601 .

Karin, M., Y. Cao, F.R. Greten, and Z.W. Li. 2002. NF-kappaB in cancer: from innocent bystander to major culprit. *Nat. Rev. Cancer.* 2:301–310.

Kato, Y., V.V. Kravchenko, R.I. Tapping, J.H. Han, R.J. Ulevitch, and J.D. Lee. 1997. BMK1/ERK5 regulates serum-induced early gene expression through transcription factor MEF2C. *EMBO J.* 16:7054–7066.

Kato, Y., R.I. Tapping, S. Huang, M.H. Watson, R.J. Ulevitch, and J.D. Lee. 1998. Bmk1/Erk5 is required for cell proliferation induced by epidermal growth factor. *Nature.* 395:713–716.

Laoukili, J., M.R. Kooistra, A. Bras, J. Kauw, R.M. Kerkhoven, A. Morrison, H. Clevers, and R.H. Medema. 2005. FoxM1 is required for execution of the mitotic programme and chromosome stability. *Nat. Cell Biol.* 7:126–136.

Lee, J.D., R.J. Ulevitch, and J. Han. 1995. Primary structure of BMK1: a new mammalian map kinase. *Biochem. Biophys. Res. Commun.* 213:715–724.

Liu, L., J.E. Cavanaugh, Y. Wang, H. Sakagami, Z. Mao, and Z. Xia. 2003. ERK5 activation of MEF2-mediated gene expression plays a critical role in BDNF-promoted survival of developing but not mature cortical neurons. *Proc. Natl. Acad. Sci. USA.* 100:8532–8537.

Liu, Z.G., H. Hsu, D.V. Goeddel, and M. Karin. 1996. Dissection of TNF receptor 1 effector functions: JNK activation is not linked to apoptosis while NF-kappaB activation prevents cell death. *Cell.* 87:565–576.

Mehta, P.B., B.L. Jenkins, L. McCarthy, L. Thilak, C.N. Robson, D.E. Neal, and H.Y. Leung. 2003. MEK5 overexpression is associated with metastatic prostate cancer, and stimulates proliferation, MMP-9 expression and invasion. *Oncogene.* 22:1381–1389.

Minella, A.C., J. Swanger, E. Bryant, M. Welcker, H. Hwang, and B.E. Clurman. 2002. p53 and p21 form an inducible barrier that protects cells against cyclin E-cdk2 deregulation. *Curr. Biol.* 12:1817–1827.

Mistry, P., K. Deacon, S. Mistry, J. Blank, and R. Patel. 2004. NF-kappaB promotes survival during mitotic cell cycle arrest. *J. Biol. Chem.* 279:1482–1490.

Mulloy, R., S. Salinas, A. Philips, and R.A. Hipskind. 2003. Activation of cyclin D1 expression by the ERK5 cascade. *Oncogene.* 22:5387–5398.

Nilsson, I., and I. Hoffmann. 2000. Cell cycle regulation by the Cdc25 phosphatase family. *Prog. Cell Cycle Res.* 4:107–114.

Nurse, P. 2000. A long twentieth century of the cell cycle and beyond. *Cell.* 100:71–78.

Pearson, G., J.M. English, M.A. White, and M.H. Cobb. 2001. ERK5 and ERK2 cooperate to regulate NF-kappaB and cell transformation. *J. Biol. Chem.* 276:7927–7931.

Piaggio, G., A. Farina, D. Perrotti, I. Manni, P. Fuschi, A. Sacchi, and C. Gaetano. 1995. Structure and growth-dependent regulation of the human cyclin B1 promoter. *Exp. Cell Res.* 216:396–402.

Pines, J., and T. Hunter. 1990. p34cdc2: the S and M kinase? *New Biol.* 2:389–401.

Ranganathan, A., G.W. Pearson, C.A. Chrestensen, T.W. Sturgill, and M.H. Cobb. 2006. The MAP kinase ERK5 binds to and phosphorylates p90 RSK. *Arch. Biochem. Biophys.* 449:8–16.

Renard, C.B., B. Askari, L.A. Suzuki, F. Kramer, and K.E. Bornfeldt. 2003. Oleate, not ligands of the receptor for advanced glycation end-products, promotes proliferation of human arterial smooth muscle cells. *Diabetologia.* 46:1676–1687.

Schouten, G.J., A.C. Vertegaal, S.T. Whiteside, A. Israel, M. Toebes, J.C. Dorsman, A.J. van der Eb, and A. Zantema. 1997. IkappaB alpha is a target for the mitogen-activated 90 kDa ribosomal S6 kinase. *EMBO J.* 16:3133–3144.

Shalizi, A., M. Lehtinen, B. Gaudilliere, N. Donovan, J. Han, Y. Konishi, and A. Bonni. 2003. Characterization of a neurotrophin signaling mechanism that mediates neuron survival in a temporally specific pattern. *J. Neurosci.* 23:7326–7336.

Wang, C.Y., M.W. Mayo, and A.S. Baldwin. 1996. TNF- and cancer therapy-induced apoptosis: potentiation by inhibition of NF-kappa B. *Science.* 274:784–787.

Wang, D., S.D. Westerheide, J.L. Hanson, and A.S. Baldwin Jr. 2000. Tumor necrosis factor alpha-induced phosphorylation of RelA/p65 on Ser529 is controlled by casein kinase II. *J. Biol. Chem.* 275:32592–32597.

Wang, X., and C. Tournier. 2006. Regulation of cellular functions by the ERK5 signalling pathway. *Cell. Signal.* 18:753–760.

Wang, X., A.J. Merritt, J. Seyfried, C. Guo, E.S. Papadakis, K.G. Finegan, M. Kayahara, J. Dixon, R.P. Boot-Handford, E.J. Cartwright, et al. 2005. Targeted deletion of mek5 causes early embryonic death and defects in the extracellular signal-regulated kinase 5/myocyte enhancer factor 2 cell survival pathway. *Mol. Cell. Biol.* 25:336–345.

Wang, Y., B. Su, and Z. Xia. 2006. Brain-derived neurotrophic factor activates ERK5 in cortical neurons via a Rap1-MEKK2 signaling cascade. *J. Biol. Chem.* 281:35965–35974.

Watson, F.L., H.M. Heerssen, A. Bhattacharyya, L. Klesse, M.Z. Lin, and R.A. Segal. 2001. Neurotrophins use the Erk5 pathway to mediate a retrograde survival response. *Nat. Neurosci.* 4:981–988.

Xia, Z., M. Dickens, J. Raingeaud, R.J. Davis, and M.E. Greenberg. 1995. Opposing effects of ERK and JNK-p38 MAP kinases on apoptosis. *Science.* 270:1326–1331.

Zhou, G., Z.Q. Bao, and J.E. Dixon. 1995. Components of a new human protein kinase signal transduction pathway. *J. Biol. Chem.* 270:12665–12669.